

See discussions, stats, and author profiles for this publication at: <https://www.researchgate.net/publication/340021072>

Inexpensive and Versatile Paper-Based Platform for 3D Culture of Liver Cells and Related Bioassays

Article in ACS Applied Bio Materials · March 2020

DOI: 10.1021/acsabm.0c00237

CITATIONS
9

READS
531

7 authors, including:



Tarun Agarwal
Indian Institute of Technology Kharagpur

92 PUBLICATIONS 1,143 CITATIONS

[SEE PROFILE](#)



Pratik Biswas
Indian Institute of Technology Kharagpur

2 PUBLICATIONS 9 CITATIONS

[SEE PROFILE](#)



Sampriti Pal
Indian Institute of Technology Kharagpur

2 PUBLICATIONS 9 CITATIONS

[SEE PROFILE](#)



Tapas Maiti
Indian Institute of Technology Kharagpur

380 PUBLICATIONS 8,383 CITATIONS

[SEE PROFILE](#)

Some of the authors of this publication are also working on these related projects:



Mechanical stress-induced autophagy in cancer metastasis [View project](#)



Hydrodynamics in microconfinements with biomimetic walls [View project](#)

Inexpensive and Versatile Paper-Based Platform for 3D Culture of Liver Cells and Related Bioassays

Tarun Agarwal, Pratik Biswas, Sampriti Pal, Tapas Kumar Maiti,* Suman Chakraborty, Sudip Kumar Ghosh, and Riddhiman Dhar



Cite This: <https://dx.doi.org/10.1021/acsabm.0c00237>



Read Online

ACCESS |

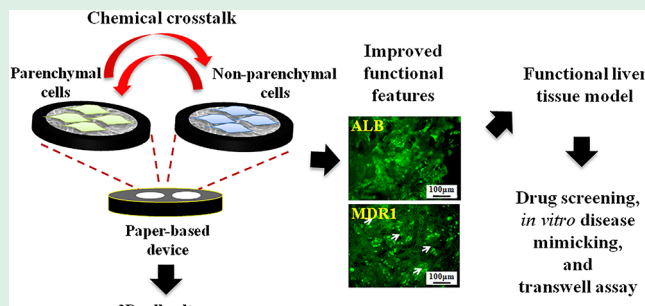
Metrics & More

Article Recommendations

Supporting Information

ABSTRACT: The present study delineates the fabrication of paper-based devices for culturing liver cells and developing related bioassays. The devices were prepared by conventional lab-based LaserJet printing technology and employed for 3D cell culture. Our results demonstrated that the devices efficiently supported the growth of multiple cell types including HepG2, HUVEC, fibroblasts, and MSCs. We further showed that the device specifications (grade of paper or design parameters) greatly impacted the functional phenotype of the HepG2 cells. We also explored the application of the developed devices for routine cell culture, drug screening, coculture, and transwell migration assays. The cellular responses observed on the paper under different culture configurations were similar to those obtained in the case of tissue culture plate (TCP). Moreover, we showed that the paper-based devices were compatible with the immunocytochemistry and ELISA procedures (no indication of nonspecific matrix-antibody interaction). Considering the simplicity, experimental flexibility, cost-effectiveness, and multiplexibility of the paper-based liver models, it is deemed to be ideal for developing cell-based bioassays, especially in resource-limited settings.

KEYWORDS: liver, filter paper, coculture, drug screening, transwell assay



1. INTRODUCTION

The current market in the field of healthcare and diagnostics demands the development of simple, portable, experimentally flexible 3D platforms for liver cell-based assays intended for multifaceted applications such as drug screening, invasion assays, molecular analysis (both protein and gene expression analysis), coculture, development of disease models, and addressing relevant biological questions about liver physiology.¹ However, the high sensitivity of the liver cells to the culture environment poses a serious limitation.^{2,3} In the absence of an optimal culture environment, the hepatocytes undergo dedifferentiation (reduction in the transcription of liver-specific genes) and lose their mature and functional characteristics. Coculture with other cell types and modulation in the architectural aspects of the substrates have been shown to result in significant improvement in the physiological behavior of the hepatocytes.^{1,3}

Various 2D and 3D liver models composing of mono- or coculture setups such as 2D transwell insert-based, cell spheroids/organoids, sandwich cultures, tissue-engineered constructs, micropatterned liver models, and liver-on-a-chip models have been developed.^{1,4,5} However, high-cost involvement, handling difficulties, and requirement of sophisticated instrumentation and skilled personnel limit their utility.^{1,6,7} In addition, the applicability of platforms is often limited to one or

other cell-based assays such as coculture of various cell types,^{8,9} Transwell migration assays,¹⁰ and drug screening.⁷ Besides this, most these platforms involve 2D cell culture methodology which are associated with significant loss of hepatocyte functionality over time of culture.^{5,11}

In this regard, the paper has come up as a promising alternative. The paper consists of randomly three-dimensionally arranged cellulose fibrils to form a porous matrix of $<200\text{ }\mu\text{m}$ thickness.^{12,13} Moreover, the features such as biocompatibility, cost-effectiveness, easy availability, passive mass-transport (via capillary action in the micron level dimensionality), suitability to chemical and physical modifications, and flexible nature have led to its vast exploration in the field of biomedical engineering.^{12,13} Over the past few years, the paper matrix has been for the development of various cell-based assays including in-cell ELISA,^{14,15} cell migration/invasion assay,^{16–20} drug screening,^{21–28} cellular cross-talk,²⁹ and solute release quantification.³⁰ To the best of our knowledge, there exist only a few studies

Received: March 2, 2020

Accepted: March 18, 2020

Published: March 18, 2020

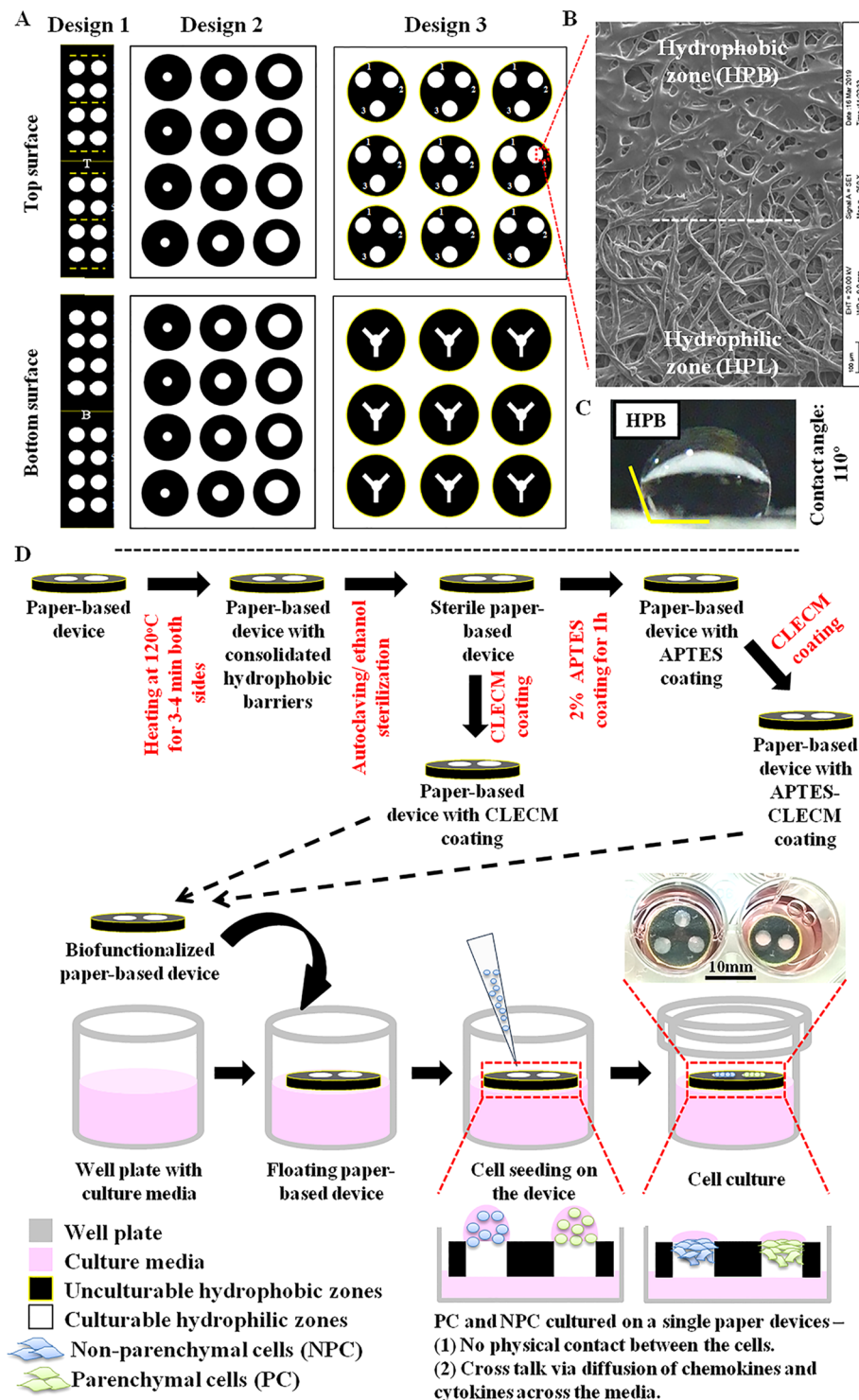


Figure 1. Design, fabrication, and application of paper-based devices. (A) Design of the fabricated paper devices. (B) Scanning electron micrographs of the fabricated paper device demonstrating the interface between the hydrophobic black and hydrophilic white zone. (C) Water contact angle measurement of the paper at the hydrophobic black zone. (D) Schematics demonstrating the preparation methodology followed for its cell culture application.

pertaining to the culture of liver cells on the paper,^{26,27,29,31} and only a single study that addresses the impact of 3D paper matrix on the hepatocyte functionality with an aim toward the development of the functional liver tissue coculture model on paper chip.²³ However, these studies do not probe into the aspects of the high-throughput requirement of bioassay

development and therefore have only limited implications from a practical perspective.

With this perspective in mind, we have fabricated paper-based devices for 3D cell culture and related bioassays using simple double-sided LaserJet printing methodology. Further, we comprehensively assessed the performance of the paper-based devices to support the culture of the HepG2 cells, both in mono-

and coculture formats, and employed them for drug screening and transwell migration assays. Moreover, we also tried to ascertain the impact of paper substrate grade and device design criterion on the cellular functionality, for which only a limited information is currently available.

2. MATERIALS AND METHODS

2.1. Materials. Whatman filter papers (grade 4 or 6) were procured from Whatman, India. Acetaminophen, Valproic acid, APTES, and SIGMAFAST DAB with metal enhancer were bought from Sigma-Aldrich, India. RPMI 1640 medium, Minimum Essential Medium (MEM), Dulbecco's Modified Eagle Medium (DMEM), fetal bovine serum (FBS), antibiotic–antimycotic solution, Trypsin-EDTA, sodium pyruvate, non-essential amino acid solution (NEAA), and MTT were purchased from Himedia, India. Phenol red-free M200 media, low serum growth supplement (LGS), GlutaMAX, calcein-AM, and ethidium homodimer were purchased from Invitrogen, India. Albumin ELISA kit was procured from Ray Biotech Life, Georgia, USA. Umbilical cord-derived mesenchymal stem cells (MSC) and human umbilical cord endothelial cells (HUVEC) were procured from Himedia, India. HepG2 cell line was obtained from National Center for Cell Science, Pune, India.

2.2. Methods. *2.2.1. Fabrication of Paper-Based Devices.* The devices were fabricated following the double-sided LaserJet printing technique as previously described by Kar et al.³² In brief, the desired design of the device was first created in Microsoft- PowerPoint software, followed by double-sided printing onto a filter paper matrix using a printer (HP LaserJet 500 Color M551). The devices were printed such that the designs on both the sides overlap onto each other. Further, the printed devices were heated for 3–4 min at 120 °C on either side to create a uniform hydrophobic barrier along the width of the paper matrix. Precautions were taken to prevent damage to the paper matrix due to the overexposure of such high temperatures. The devices thus formed had hydrophilic culturable white zones separated by black hydrophobic zones. The formation of the hydrophobic zones in the device was validated by measuring the contact angle. The morphological characteristics of these zones were visualized using scanning electron microscopy (ZEISS). Prior to imaging, the devices were sputter-coated with gold and then visualized at 20 kV voltage. The culturable zones were further biofunctionalized with Caprine liver-derived extracellular matrix (CLECM) (200 µg/mL, following either direct coating or APTES-mediated coating methodology as reported elsewhere^{11,13}). In our work, we fabricated three different formats of the devices intended for a specific application: Design 1, for routine cell culture, immunocytochemistry, in-cell ELISA, drug screening, and coculture assays; Design 2, for optimization assays; and Design 3, for transwell migration assay (**Figure 1A**).

2.2.2. Cell Maintenance. In this study, we worked with four different cells, namely HepG2, MSC, HUVEC, and MDF. HepG2 cells were cultured in MEM, MSC in RPMI 1640, and MDF in DMEM (with 1× GlutaMAX, 1× NEAA, and 1× sodium pyruvate) media. All the media were supplemented with 10% FBS, 1× antibiotic–antimycotic solution. HUVEC was cultured in phenol red-free M200 supplemented with 1× LGS and 1× antibiotic–antimycotic solution. All the cells were maintained at 37 °C, 5% CO₂ incubator with 90–95% humidity during the culture period. Mouse dermal fibroblast (MDF) cells were isolated from Swiss Albino mouse as described elsewhere³³ with permission by the Institutional Animal Ethics Committee (IAEC), Indian Institute of Technology (IIT) Kharagpur (878/IAEC/15). All the primary cells were used within passage number 3–5.

2.2.3. Cell Seeding and Culture on Paper Devices. The procedure followed for cell seeding on the paper device has schematically been demonstrated in **Figure 1D**. In brief, the sterile biofunctionalized paper devices were first floated onto 400 µL of culture media surface in a 24-well plate and allowed to equilibrate for the next 10–15 min. After that, the cells were seeded in the hydrophilic zone of the devices at a density of 7.5 × 10³ cells/slot. The complete setup was placed in a CO₂ incubator, cultured, and further applied for the desired application.

For all the experiments, the cell viability was determined by standard MTT assay followed by spectrophotometric evaluations. For this, the paper devices were incubated in MTT solution (0.4 mg/mL in incomplete MEM) for 1.5 h. Thereafter, the devices were retrieved, bottled off for excess of spent media and placed in eppendorf containing 400 µL of DMSO to dissolve the formazan crystals. The optical density of the solutions was evaluated using a UV–visible spectrophotometer at 595 nm. If required, each culturable slot of the paper device could be segregated and assessed of the amount of MTT metabolized following the same methodology. The viable cell population on the paper devices was further visualized by fluorescence microscopy (Olympus IX71) after calcein-AM/ethidium homodimer staining.

The functional aspects of the cultured HepG2 cells were estimated using ELISA and EROD assay. For ELISA, the HepG2 cells were cultured on devices as described above, followed by retrieval of the spent media and estimation of secreted albumin using human-specific albumin ELISA kit as per the manufacturer's instructions. For EROD assay, the cells were cultured on the paper matrix, as mentioned above. Thereafter, the spent media were replaced with phenol red-free media containing 2% FBS, 7-ER (2 µM), and dicumarol (10 µM). The setup was incubated for 3 h in a CO₂ incubator. The reaction was stopped by diluting the supernatant in methanol, and the amount of 7-ER metabolized was estimated using a spectrofluorometer (Fluoromax-4, Horiba Scientific). The data were normalized with the MTT values of the corresponding set.

2.2.4. Drug-Induced Liver Injury (DILI) Model on Paper. For this, we evaluated the cell toxicity in response to two commonly known hepatotoxins acetaminophen (APAP) and valproic acid (VPA) on 3D-paper devices. In brief, HepG2 cells were seeded onto each slot of the paper device, as described in **Section 2.2.3**. The complete setup was placed in a CO₂ incubator and cultured for 7 days. After that, the spent media were replaced by the fresh media containing APAP (15 mM) or VPA (12 mM) and incubated for another 48 h. Cell viability was estimated by MTT assay, as described in **Section 2.2.3**. A similar study was carried out on a 2D culture plate as a control.

2.2.5. Indirect Coculture Studies on Paper Device. For this, the HepG2 cells were cultured on the paper devices as described in **Section 2.2.3**. On the fifth day, the devices were transferred to another well of a 24-well plate individually containing 1.5 × 10⁴ nonparenchymal cells (NPC; either MSC or HUVEC or MDF). Under coculture setting, the cells were maintained in culture media containing two parts of PC-specific media and one part of NPC-specific media at 37 °C in a 5% CO₂ incubator for another 72 h. The control, monoculture system did not contain any cells in the bottom well and was maintained in the same media (as used for coculture). Alterations in the albumin secretion profiles were estimated using human-specific albumin ELISA as described earlier.

Normalization of albumin data was carried out with the MTT values of the HepG2 cells of the corresponding set. For this, only the paper devices were used for quantification as described earlier.

Further we also evaluated APAP toxicity on paper-based devices under coculture conditions. For this, the devices (with HepG2 cells cultured for 5 days) were transferred in a well plate containing NPCs (at the bottom of the well). The cocultured system was first maintained for 24 h, followed by treatment with 10 mM APAP for 48 h. Cell viability was estimated by quantifying the MTT values of HepG2 cells as described above.

2.2.6. Transwell Migration Assay on Paper. For this, NPCs (2 × 10⁴ cells) were seeded onto each slot of the paper-based device (design 3), as described in **Section 2.2.3**, while the parenchymal HepG2 cells (~5 × 10⁴ cells) were seeded in a 24-well plate as a 2D culture. The cells were maintained in culture media containing two parts of PC-specific media and one part of NPC-specific media at 37 °C in a 5% CO₂ incubator. The migration of NPCs to the bottom of the paper device was visualized by fluorescence microscopy post-calcein-AM staining under different culture configurations. The quantification of the cell migration was done by manual counting the number of cells at the base of the devices.

2.2.7. Statistical Analysis. All the experiments were conducted in triplicates (unless otherwise mentioned), and data were represented as

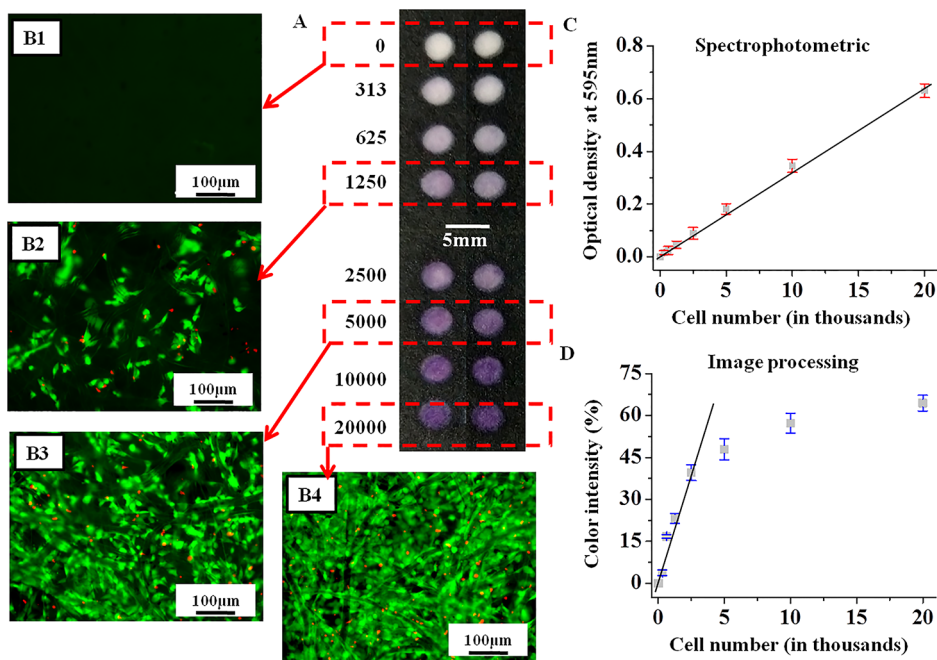


Figure 2. Paper-based device for HepG2 cell culture. (A) Representative images of the paper device seeded with a variable number of cells after MTT assay. (B1–B4) Fluorescent micrographs positive/dead staining of the paper devices seeded with a variable number of cells. MTT color intensities versus cell number evaluation using (C) UV-visible spectrophotometry and (D) image processing tools. All the evaluations were carried out in triplicate ($N = 3$).

mean \pm standard deviation. The statistical significance of the data was analyzed using Origin Pro 8.0 software with a 95% confidence interval.

3. RESULTS AND DISCUSSION

3.1. Preparation and Characterization of Paper-Based Devices.

Recently, paper matrixes have widely been explored for cell culture and related applications.³⁴ However, direct usage of the paper matrix could result in a non-uniform cell spreading due to its superhydrophilic and high wicking nature.^{35,36} For this, the researchers have employed methodologies such as wax printing,^{15,16,24} Teflon printing,³⁵ PDMS stenciling,^{37,38} heat pressing,¹⁷ chemical modification,³⁹ and combine extrusion printing with layer-by-layer lamination (ExCeL)⁴⁰ to develop hydrophobic barriers. This would restrain cells within the specified hydrophilic culturable zones. In the present work, we have alternatively applied a printing methodology involving the use of traditional lab LaserJet printers for the same (Figure 1A). Scanning electron micrographs of the printed paper matrix revealed the presence of a smooth coating over the printed hydrophobic zones, while the hydrophilic zones showed no such alterations (clearly visible cellulose fibrils were present) (Figure 1B). Contact angle measurements also validated the hydrophobic nature (contact angle: 110°) of the printed black zones (Figure 1C). Interestingly, we observed that the printed devices experienced high surface tension at the liquid–paper interface (due to their hydrophobic nature) and floated over the liquid surface. Thus, in the present study, we exploited this feature of the devices to establish the floating paper-based cell culture methodology for the first time.

To improve the biological aspects of the devices, the culturable white zones were biofunctionalized with CLECM. CLECM is a complex mixture of liver ECM components derived from a caprine source, which could provide biochemical cues to the hepatocytes, necessary for their growth and functionality

maintenance.¹¹ Notably, either direct coating or APTES-mediated coating¹³ methodology could be opted for the same.

Also, it is important to mention that the devices were compatible with high-temperature baking (checked up to 130 °C), standard autoclaving procedures, sterilization with ethanol, and various biofunctionalization procedures. Notably, these procedures did not cause any ink bleeding into hydrophilic culturable zones (refer to Figure S1).

3.2. HepG2 Cell Culture on Paper-Based Devices. We first seeded a variable number of HepG2 cells on the paper device and cultured them for 24 h followed by MTT assay. The results revealed that the cells on the paper devices could metabolize MTT, thereby providing a hint regarding their viability and metabolic activity. Moreover, similar to traditional plate-based culture systems, the amount of formazan crystals formed on the paper devices was dependent on the number of cells seeded onto each slot (Figure 2A). Notably, the selection of the methodology (spectrophotometric or image processing-based) for the quantification of metabolized MTT is also crucial. In the case of the conventional method (involving the dissolution of formazan crystals in DMSO, followed by spectrophotometric evaluation), we observed a linear correlation between the cell number and the amount of MTT metabolized (Figure 2C). On the contrary, such linearity was severely compromised (limited at only lower cell numbers) in the case of the image-based analysis (Figure 2D). This could be attributed to the 3D distribution of cells and the limitations of the capturing tools.

Further, the live/dead assay also demonstrated the presence of a viable cell population with a minimal dead cell population even at higher cell concentrations (Figure 2B). Visually, the individual cells could be spotted in the slots seeded with low cell numbers, while those containing high cell numbers formed a cellular sheet along the surface of the paper fibrils. Further extension of the culture duration also did not impact the viability

of the cells, thereby suggesting the nontoxic nature of the paper and the printing ink. Notably, the presence of a viable cell population even after 7 days of culture also provides a hint that the floating methodology (as opted herein) did not negatively impact the growth of cells. This could be attributed to (i) humidified environment in the CO₂ incubator, which slows down the evaporation rate, (ii) regular media changes (within 48–72 h), and (iii) high mass transfer coefficient and wicking potential of the paper matrix.

3.3. Optimizing Paper Devices for HepG2 Cell Culture.

Hepatocytes are very sensitive, and the absence of a suitable microenvironment (including matrix topology and architecture) results in significant alterations in their phenotypes. To the best of our knowledge, there is no report available that addresses the impact of paper matrix specifications and design parameters on the physiology of the hepatocytes. With this perspective, we fabricated paper devices on different grades of paper (grade 4 and 6) along with different design parameters (device 2, Figure 1A) of the culturable area and assess their impact on HepG2 cell behavior.

3.3.1. Effect of Design Parameters of Paper Device on HepG2 Cell Functionality. For this, we first prepared devices on G4 paper with different diameters of the culturable zones, namely 5.0, 3.5, and 2.0 mm that significantly imparts variation in the culturable volume on the paper matrix. The volume available for the cells on D5.0, D3.5, and D2.0 devices would correspond to ~15.70, 7.69, and 2.51 mm³, respectively (Figure 3A). We further seeded an equal number of cells (7.5×10^3 cells) onto the culturable zones and subjected the setup to floating culture for 7 days.

The results demonstrated that cell proliferation was greatly influenced by available culturable volume on the paper matrix with D5.0 supporting the highest proliferation followed by D3.5 and D2.0 devices (Figure 3B). On day 4, the MTT values on D5.0 and D3.5 were ~2.2- and ~1.71-fold higher than D2.0 devices, respectively ($p < 0.05$). Notably, ~1.31-, ~1.44-, and ~1.64-fold increases in the MTT values were observed in the case of day seven cultures as compared to day 4 ($p < 0.05$). In addition, the live/dead assay also revealed that lower proliferative potentials of the cells, as observed in the case of D2.0, were not attributed to the decrease in the cell viability (refer to Figure S3A in the supporting file).

Evaluation of albumin secretion revealed that at day 4, the cells cultured in the confined matrix volume, that is, the D2.0 device exhibited the highest albumin secretion followed by D3.5 (~1.29-fold lower) and D5.0 (~1.78-fold lower) sets ($p < 0.05$) (Figure 3C, Note S2). Upon further increase in the culture duration, the cells on all the devices showed a significant reduction in the albumin secretion levels. Interestingly, the D2.0 devices (with smaller confinement) significantly prolonged such a loss in the cellular functionality. The observed albumin secretion on D2.0, D3.5, and D5.0 devices was ~0.89-, ~0.74-, and ~0.66-fold, respectively, on day 7 with reference to day 4. Such a variation in the cellular response could be explained in terms of cellular densities. The cells in the D2.0 devices with confined culture volumes have a higher density that allows them to undergo better cell–cell interaction that positively modulates their functional state. On the other hand, in the case of the D5.0 device, a dispersed distribution of the cells makes them more prone to migration and dedifferentiation (loss of hepatic functionality).

Interestingly, unlike the albumin secretion, we observed that the cells cultured on D5.0 exhibited significantly higher EROD

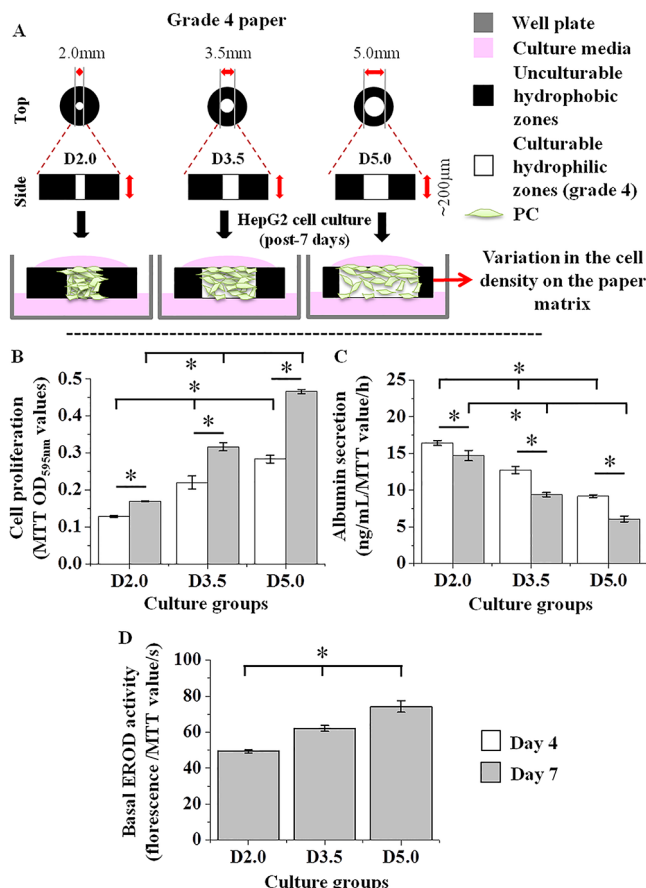


Figure 3. Effect of the diameter of the culturable zone of paper devices on cell phenotype. (A) Schematic representation of HepG2 cell culture on paper devices with different diameters of culturable zones. (B) Cell proliferation analysis on paper devices with different diameters of culturable zones. (C) Albumin secretion by the cells cultured on paper devices with different diameters of culturable zones. (D) EROD activity of the cells cultured on paper devices with different diameters of culturable zones. All the evaluations were carried out in triplicate ($N = 3$). * represents a significant difference among the groups with $p < 0.05$.

activity followed by D3.5 and D2.0 devices (Figure 3D, Note S2). The EROD values on D5.0 and D3.5 were ~1.77- and ~1.21-fold higher as compared to D2.0 devices, respectively ($p < 0.05$). This could be attributed to the higher cell proliferation and infiltration of the cells into the paper matrix in the case of D5.0 devices, which would result in the induction of a local hypoxic environment and thus eliciting the EROD activity of the cells. Previous reports have already linked hypoxia as a positive modulator of cytochrome P450 activity in the hepatocytes, including HepG2 cells.⁴¹ On the other hand, in the case of D2.0 devices, although the relative cell density is higher as compared to D3.5 or D5.0, yet lower cell numbers could limit the formation of hypoxic zones and showed lower EROD activity.

In a study, Nishikawa et al. also reported a similar observation wherein the HepG2 cell spheroid with smaller sizes exhibited higher albumin secretion, while those with larger sizes showed better EROD activity (linked to the development of hypoxic regions in larger spheroids).⁴²

3.3.2. Effect of Paper Grade on HepG2 Cell Functionality. Furthermore, the variations in the confinements could be brought about by altering the grade of the paper matrix. With this perspective, we fabricated D3.5 devices on grade 4 (G4, pore size 20–25 μm) and grade 6 (G6, pore size 3–4 μm) paper,

followed by cell seeding (7.5×10^3 cells/zone) and floating culture for 7 days (Figure 4A) (refer to Figure S2 for SEM images).

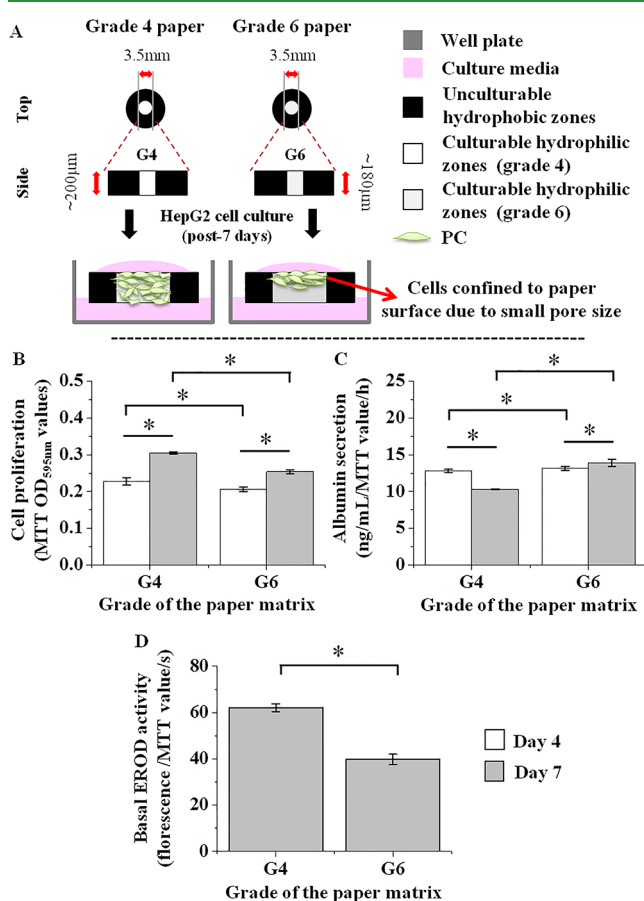


Figure 4. Effect of the grade of paper on cell phenotype. (A) Schematic representation of HepG2 cell culture on grade 4 and 6 matrixes. (B) Cell proliferation analysis on grade 4 and 6 matrixes. (C) Albumin secretion by the cells cultured on grade 4 and 6 matrixes. (D) EROD activity of the cells cultured on grade 4 and 6 matrixes. All the evaluations were carried out in triplicate ($N = 3$). * represents a significant difference among the groups with $p < 0.05$.

The experimental results revealed that the cells on the G6 matrix exhibited a lower proliferation than that on the G4 matrix (Figure 4B). The MTT values at day 7 were ~ 1.35 - and ~ 1.23 -fold higher on G4 and G6 paper matrix, respectively, with respect to day 4 cultures ($p < 0.05$). Live/dead assay also confirmed no critical impact on the cell viability, thereby suggesting that the decrease in the MTT values on G6 was not attributed to the loss of cell viability (refer to Figure S3A).

Albumin profiling suggested no significant difference in the secretion levels on either G4 or G6 matrix at day 4 ($p > 0.05$) (Figure 4C, Note S2). However, by day 7, the cells on the G4 matrix showed a reduction in albumin secretion as compared to day 4, while in the case of the G6 matrix, similar secretion levels were maintained ($p < 0.05$). These results suggested that even though the design specifications of the culturable zones were identical on both the paper types, the cells on G6 paper tended to experience a more restricted culture environment and were confined to the surface of the matrix due to their inability to infiltrate through such smaller pore sizes. Similar to the D2.0 devices (as shown in the previous section), the confined culture

environment in the case of the G6 matrix would also allow them to form better cell–cell contacts and undergo 2D/3D morphogenesis and thereby positively impart higher functional states. On the other hand, the cells on the G4 matrix infiltrated into the paper matrix (owing to the bulk diffusion of growth factors from the culture media) due to the larger pore size of the matrix and resulted in their loss of functional state. Previously, Ranucci et al. also reported a similar observation wherein the collagen scaffolds with a pore size ($< 10 \mu\text{m}$) supported a higher functional state of the hepatocytes than those with pore sizes ($\sim 20 \mu\text{m}$).⁴³

Notably, the EROD activity was higher in the case of nonconfined culture (in the case of G4 matrix) than that observed in confined culture on the G6 matrix ($p < 0.05$) (Figure 4D, Note S2). Interestingly, the alterations in the culture zone dimensions on the G6 matrix affected the cellular EROD activity in a similar way as observed on the G4 matrix (refer to Section 3.3.1). EROD activity was highest on D5.0 (G6) followed by D3.5 (G6) and D2.0 (G6) (refer to Figure S4).

3.4. Application Perspective: Paper-Based Tissue Models.

3.4.1. Hepatotoxic Responses on Paper-Based Devices. Estimation of hepatotoxic responses of the drugs is one of the most in-demand applications of the *in vitro* liver models. For this, we first fabricated the paper-based devices on G4 and G6 matrixes in all the configurations (D2.0, D3.5, and D5.0), followed by HepG2 cell culture. After that, we assessed the cytotoxic response of commonly used clinical hepatotoxins (APAP or VPA) and also compared it with traditionally used 2D cultures (Figure 5A).

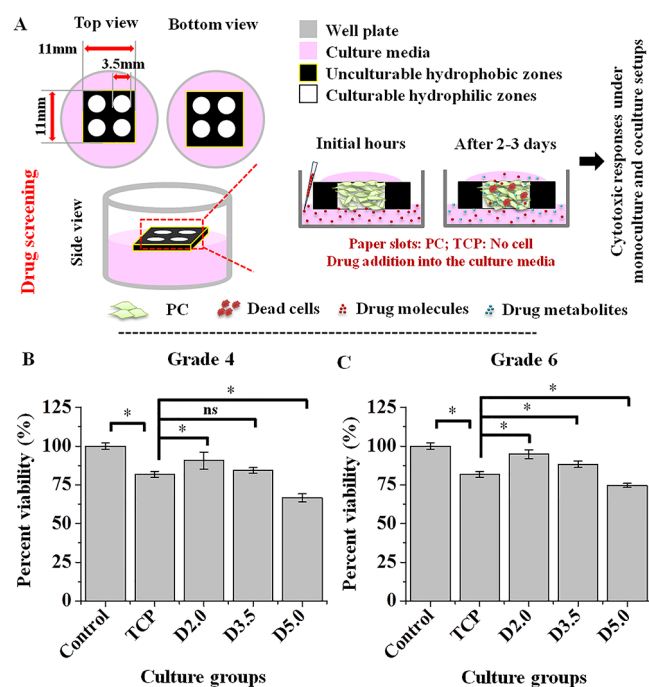


Figure 5. DILI model on paper. (A) Schematics of the paper-based drug screening assay. (B) Percentage HepG2 cell viability on G4 paper under different culture configurations upon APAP treatment. (C) Percentage HepG2 cell viability on G6 paper under different culture configurations upon APAP treatment. All the evaluations were carried out in triplicates ($N = 3$). * represents a significant difference among the groups with $p < 0.05$. ns represents a significant difference among the groups with $p > 0.05$.

The results demonstrated that the drugs exerted cytotoxicity, both in 2D (monolayer) and 3D (paper-based) culture setups, irrespective of the paper grade and design configuration. However, there existed critical differences in the observed toxicity trend among all the groups.

In the case of the APAP treated group, the cells cultured on the G4 devices with D5.0 configuration exhibited significantly higher cell death followed by D3.5 and D2.0 ($p > 0.05$) (Figure 5B). Such varied results could be attributed to the variability in the xenobiotic-metabolizing potential of the cells in the different groups. In general, APAP does not cause direct toxicity to the cells; instead, it is metabolized by Phase I enzymes (CYP1A2 or CYP2E1) expressed in the hepatocytes and gets converted to N-acetyl-p-aminobenzoquinone imine (NAPQI), which has cytotoxic effects via induction of oxidative stress.^{44–46} In our previous Section 3.3.1, we demonstrated a higher CYP1A1/2 activity on D5.0, followed by D3.5 and D2.0 configurations; thus, with this analogy, higher cell death on D5.0 could directly be linked to higher cytochrome P450 expression profiles. Another plausible reason for the same could be a higher expression of phase II and phase III (in the case of D2.0 and D3.5), which would detoxify APAP or its metabolites (via sulfation or glucuronidation) or secrete them out of the cells (through transporter activity). Confined cultures have already been shown to improve the expression of phase II and phase III proteins.⁴⁷

Interestingly, we also observed that the cells on the G6 paper matrix exhibited a similar trend in cell viability (D2.0 > D3.5 > D5.0). Comparison between the cells grown on the different grade of paper matrix demonstrated that on G4 matrix (nonconfined cultures), cells were more susceptible to APAP than in the case of G6 (confined cultures), irrespective of their design specifications (Figure 5C). Notably, D2.0 and D3.5 configurations on the G4/G6 matrix showed insignificant variation in cell viability (refer to Figure S5A). In addition, cell death observed in the case of 2D monolayer cultures was higher than D2.0 and D3.5 while lower than the D5.0 configuration. This could be attributed to the difference in the drug-metabolizing potential of the cells under different culture configurations.

In the case of VPA, we observed a similar trend; however, cell death observed in the 2D monoculture system was lesser than that observed on paper matrix irrespective of grade or design configurations (details mentioned in the supporting file, Figure S5B).

3.4.2. Coculture on Paper-Based Devices. Under native conditions, the hepatocytes interact with multiple other hepatic cells including hepatic sinusoidal endothelial cells, stellate cells, Kupffer cells, cholangiocytes, and stem cells.^{3,4,23} These interactions together modulate overall functionality at the tissue level.^{1,3} *In vitro* also, the interaction between these cell types has been shown to impact the proliferation, migration, maturation, and drug metabolism.^{1,48–50} With this perspective, we, herein, have tried to evaluate the potential of the paper-based device for the development of liver coculture models.

For this, we cocultured HepG2 cells with different NPCs, including HUVEC, MDF, and MSCs, on paper devices (design 1) and studied an individual effect of each NPC cell type on the albumin secretion profile of the HepG2 cells (Figure 6A). Notably, we opted for indirect coculture methodology, wherein PC were cultured on paper devices and NPCs at the base of a 24-well plate. Under such conditions, there existed no direct contact

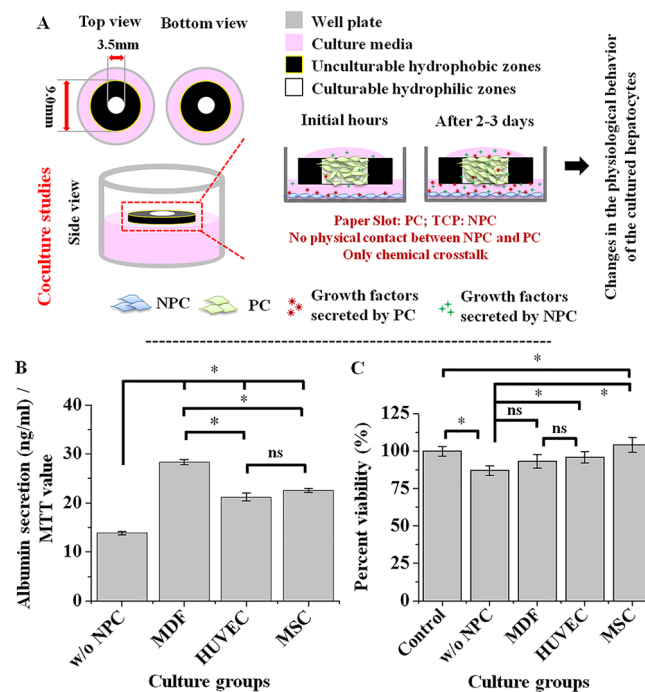


Figure 6. Coculture model on the paper. (A) Schematics of the liver-based coculture model on the paper. (B) Albumin secretion by HepG2 cells in monoculture and coculture with MDF, HUVEC, and MSCs on paper. (C) Percentage HepG2 cell viability in monoculture and coculture with MDF, HUVEC, and MSCs upon treatment with APAP. All the evaluations were carried out in triplicate ($N = 3$). * represents a significant difference among the groups with $p < 0.05$. ns represents an insignificant difference among the groups with $p > 0.05$.

between both the cell types, however the exchange of soluble factors was possible.

The analysis showed ~2.046-, 1.529-, and 1.627-fold increase in albumin secretion by HepG2 cells after 72 h of coculture with MDF, HUVEC, and MSCs, respectively, as compared to monoculture systems ($p < 0.05$) (Figure 6B). This could be attributed to the chemical crosstalk between PCs and NPCs and further activation of multiple signaling cascades. Similar results have already been reported for coculture between HepG2 cells and fibroblasts^{51,52} or endothelial cells^{53,54} or mesenchymal stem cells^{55–57} in various other culture models. Wang et al. reported a similar hepatocyte response under coculture with endothelial cells on the paper matrix.²³ Moreover, a critical difference in the HepG2 proliferation under coculture and monoculture setup was also observed (refer to Figure S6).

We further assessed APAP toxicity under coculture conditions (Figure 6C). The results demonstrated that the HepG2 cells had lower susceptibility toward APAP in the coculture groups as compared to the monoculture ones. The percentage decrease in cell viability in the monoculture was ~12.87%, while the same in case of coculture with MDF and HUVEC was ~7.22 and ~4.08%, respectively. On the contrary, HepG2 cells cocultured with MSCs showed an increase in cell viability by 4.14% with respect to untreated systems. This could be due to the hepatoprotective effects imparted by the NPCs by reducing the oxidative stress upon APAP treatment to the hepatocytes. Similar results have been previously reported elsewhere.^{53,54,58–60}

Together, these results suggest that paper-based 3D culture could effectively support the development of coculture systems.

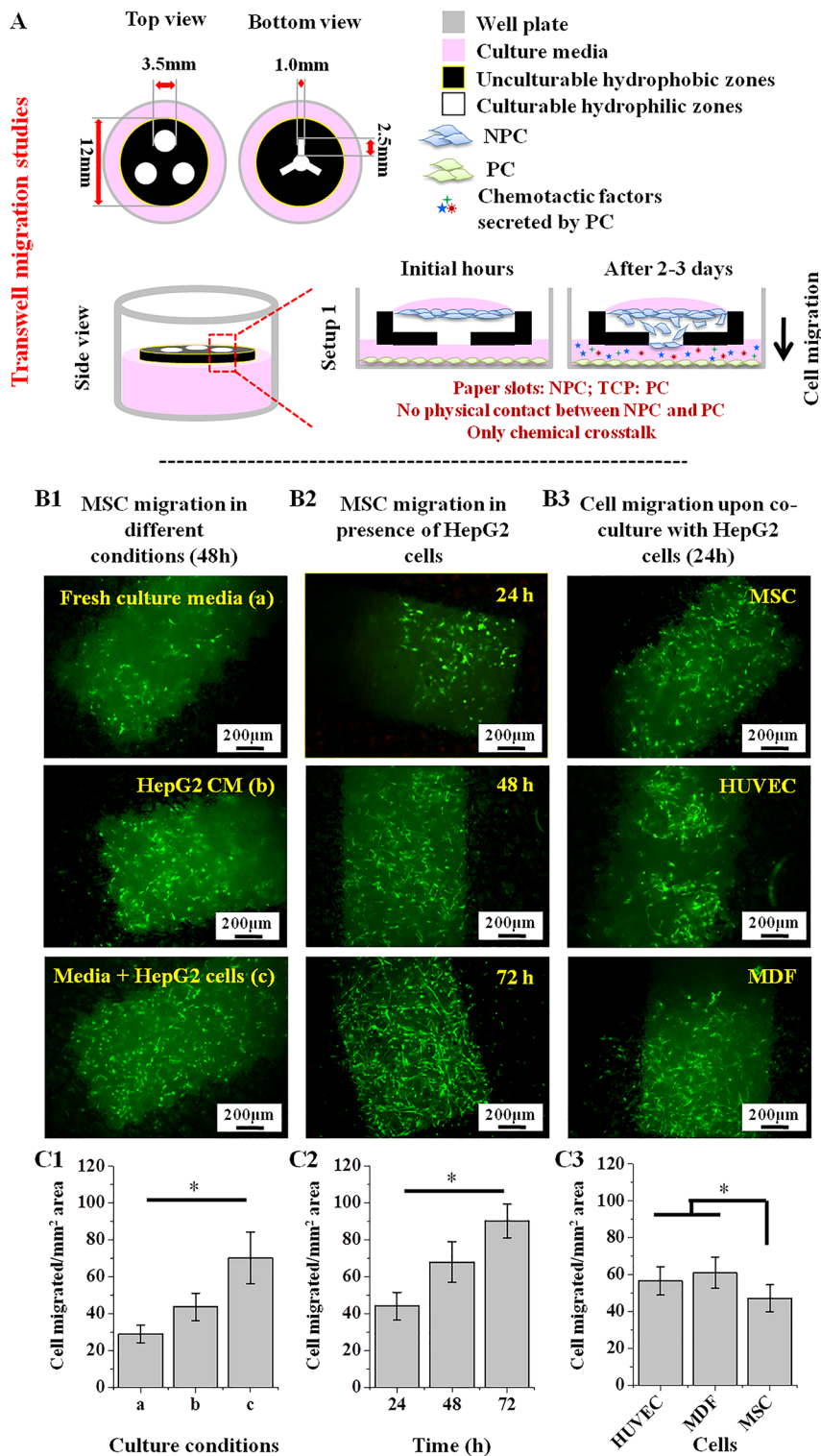


Figure 7. Transwell migration assay on paper. (A) Schematics of the paper-based Transwell migration assay. (B1–B3) Representative fluorescent images of the migration of NPCs population when exposed to different culture conditions. (C1–C3) Quantification of the cell migration of NPC population when exposed to different culture conditions using the fluorescent micrographs. All the evaluations were carried out in triplicate ($N = 6$). * represents a significant difference among the groups with $p < 0.05$.

3.4.3. Transwell Migration Assay on Paper-Based Devices. Cell migration is a phenomenon where a cell migrates from one point to another under the influence of chemotactic factors.⁶¹ In vivo, such phenomenon allows the body to tackle infections or injuries and further facilitate tissue repair and regeneration.^{61,62} In vitro, the cells have also been shown to retain such migratory

responses in the presence of chemotactic agents.¹⁶ With this perspective, we tried to evaluate the potential of our paper-based device to support cell migration/invasion assays under different experimental conditions (Figure 7A). Figure S7 demonstrates the representative images of paper matrix seeded with HepG2, MDF, HUVEC, and MSCs.

In the first set of experiments, we quantified the invasion of MSC in the presence of only fresh culture media, HepG2 conditioned media, and in coculture with HepG2 cells (Figure 7B1). Herein, we used MSCs as they are often been applied to regenerative liver studies and also have good migratory potential.⁶³ The results showed that in the presence of fresh culture media (containing 10% FBS), only a few cells migrated to the bottom of the paper device. However, the addition of 50% HepG2 conditioned media or indirect coculture with HepG2 cells significantly increased the migratory potential of the MSCs by ~1.51- and 2.42-fold ($p < 0.05$). This could be attributed to the secretome of the HepG2 cells, which consists of various growth factors such as IGF1, SDF1, bFGF, VEGF, and HGF, which are known to increase the migratory potential of MSCs.^{64–66} A further increase in the MSC migratory potential in coculture as compared to the conditioned media set could be due to the following: (i) in 50% of conditioned media, all the chemoattractants are provided to the cells during the initiation of the setup (which may even degrade over time), while in a coculture setting, the cells continuously secrete the chemokines and cytokines, which would induce higher cell migration; and (ii) under coculture setting, the NPCs and the HepG2 cells both crosstalk with each other, which would further modulate their phenotype and their secretome, thereby altering the cellular migration as demonstrated elsewhere.⁶⁷ On the other hand, no such cross-talk exists in conditioned media setup.

In the second set of experiments, we quantified the migration of the MSCs cocultured with the HepG2 cells as a function of time (Figure 7B2). The results showed a significant increase in the MSCs migration to the bottom of the paper with a culture duration. MSC migration at 48 and 72 h was 1.54- and 2.04-fold higher than that observed after 24 h. This could be due to the continuous exposure of MSCs to the HepG2 secretome (the composition of the secretome could further be modulated due to the cross-talk between both the cells⁶⁷), thereby allowing more MSCs to migrate to the bottom of the paper-devices.

In our third set, apart from MSCs, we also compared the migration of other NPCs (which are essential components in liver repair and regeneration including fibroblasts and endothelial cells) in response to HepG2 coculture (Figure 7B3). The results revealed that the MDF (1.29-fold) and HUVEC (1.19-fold) cells had significantly higher migration as compared to MSCs. This could be a result of either the variation in the intrinsic migratory potential of the cells or the differences in sensitivity of the cells to the biochemical composition of the HepG2 cell secretome.

Notably, we observed a similar response in traditional Transwell assay when the NPCs were exposed to similar culture configurations (refer to Figure S8).

On the basis of these observations, we could say that the paper-based device supported the Transwell migration assay similar to the conventional platforms. However, here, it is important to mention that the cellular migration on the paper-based devices is a result of bulk diffusion of the chemokines and cytokines and could not be correlated completely to the chemotactic gradients that develop *in vivo*. A similar observation has previously been reported elsewhere.¹⁶

4. CONCLUSION

In summary, we developed simple, easy to fabricate, portable, and cost-effective paper-based devices with potential applications in developing multiple mammalian cell assays. We showed that the paper devices were biocompatible and supported both

3D mono- and coculture (with NPCs) of the HepG2 cells, thereby positively influencing their functional phenotype. We also tried to address a relevant yet unanswered question: "how could paper confinements modulate the behavior of the cultured cells?" We observed that the cells cultured in the confined spaces exhibit lower proliferation and higher functional state (in terms of albumin secretion). The EROD activity, on the other hand, was mostly linked to the formation of a local hypoxic environment and showed lesser dependence on paper confinements. Further aspects such as (i) impact of device design and patterning, (ii) culture configurations (floating v/s submerged cultures), and (iii) culture conditions (media volume and media composition) still need an in-depth evaluation and present a future scope of investigation.

Furthermore, it is also important to mention that several studies have individually exploited the paper matrix for one or another application. These studies have developed an integrated platform with paper as a substrate for tracking cell invasion, coculture, and drug screening studies, which could still be unaffordable for laboratories in resource-limited settings. On the contrary, in our study, we successfully cultured the cells on the paper devices using a simple yet efficient floating cell culture methodology. We further exploited the paper matrix for multifaceted applications just by altering the base design of the paper devices. Interestingly, the cost incurred for procuring a conventional transwell 96-well plate for coculture and transwell migration studies is ~INR 7000, which was found to significantly reduce to ~INR 200–300 in case of our paper devices (wherein the paper devices costs around INR 2, while the remaining cost was incurred by the conventional TCP used for placing the paper devices). An exact cost breakup has been provided in Table S3. We aim that such technology could be exploited within the laboratory environment, thereby overcoming the dependency on the commercially available costly consumables. Notably, the cost estimations made herein are completely restricted to laboratory scale and may not be appropriate for scale-up settings as previously suggested by Wilson et al.⁶⁸

In addition, from our previous work,¹³ its inferred that the applicability of these paper-based devices is not just restricted to liver cells but could be extended toward developing various paper-based tissue models and further addressing multiple biological questions pertaining to them, opening up new vistas in biology and engineering. Furthermore, the paper-based devices were also compatible with immunocytochemistry and ELISA procedures to detect the gene expression at the protein level without any indication of nonspecific matrix–antibody interaction (refer to Figure S9 and S10).

■ ASSOCIATED CONTENT

SI Supporting Information

The Supporting Information is available free of charge at <https://pubs.acs.org/doi/10.1021/acsabm.0c00237>.

Methods for in-cell ELISA, method for image analysis, list of antibodies used, cost-break up, images of devices after processing, representative images of grade 4 and 6 paper, representative live/dead images, cell proliferation and EROD activity of cells on different paper devices, cell viability of cells on different paper devices upon APAP and VPA treatment, cell proliferation of HepG2 cells under coculture conditions, transwell migration assay using traditional insert method, functional analysis of

HepG2 cells cultured in TCP and paper matrix, representative images of in-cell ELISA ([PDF](#))

AUTHOR INFORMATION

Corresponding Author

Tapas Kumar Maiti — Department of Biotechnology, Indian Institute of Technology, Kharagpur, West Bengal 721302, India; [orcid.org/0000-0002-3984-5911](#); Phone: +91-3222-283766; Email: tkmaiti@iitkgp.ernet.in, maitapask@gmail.com

Authors

Tarun Agarwal — Department of Biotechnology, Indian Institute of Technology, Kharagpur, West Bengal 721302, India

Pratik Biswas — Department of Biotechnology, Indian Institute of Technology, Kharagpur, West Bengal 721302, India

Sampriti Pal — Department of Biotechnology, Indian Institute of Technology, Kharagpur, West Bengal 721302, India

Suman Chakraborty — Department of Mechanical Engineering, Indian Institute of Technology, Kharagpur, West Bengal 721302, India; [orcid.org/0000-0002-5454-9766](#)

Sudip Kumar Ghosh — Department of Biotechnology, Indian Institute of Technology, Kharagpur, West Bengal 721302, India

Riddhiman Dhar — Department of Biotechnology, Indian Institute of Technology, Kharagpur, West Bengal 721302, India

Complete contact information is available at:

<https://pubs.acs.org/10.1021/acsabm.0c00237>

Author Contributions

T.K.M. and T.A. jointly designed the study. T.A. and S.P. carried out cell culture and functionality analysis. P.B. prepared the paper devices. S.C. provided the facility for device printing. T.A., S.P., and P.B. contributed to manuscript writing. T.K.M., R.D., S.K.G., and S.C. were involved in continuous work evaluation and manuscript editing.

Notes

The authors declare no competing financial interest.

ACKNOWLEDGMENTS

The authors would like to acknowledge the INSPIRE scheme, Department of Science and Technology, Government of India, for providing the fellowship to T.A. S.C. gratefully acknowledges the Department of Science and Technology, Government of India, for the Sir J. C. Bose National Fellowship.

REFERENCES

- (1) Underhill, G. H.; Khetani, S. R. Bioengineered liver models for drug testing and cell differentiation studies. *Cell Mol. Gastroenterol. Hepatol.* **2018**, *5* (3), 426–439.
- (2) Lauschke, V. M.; Hendriks, D. F.; Bell, C. C.; Andersson, T. B.; Ingelman-Sundberg, M. Novel 3D culture systems for studies of human liver function and assessments of the hepatotoxicity of drugs and drug candidates. *Chem. Res. Toxicol.* **2016**, *29* (12), 1936–1955.
- (3) Agarwal, T.; Subramanian, B.; Maiti, T. K. Liver tissue engineering: challenges and opportunities. *ACS Biomater. Sci. Eng.* **2019**, *5* (9), 4167–4182.
- (4) LeCluyse, E. L.; Witek, R. P.; Andersen, M. E.; Powers, M. J. Organotypic liver culture models: meeting current challenges in toxicity testing. *Crit. Rev. Toxicol.* **2012**, *42* (6), 501–548.
- (5) Gaskell, H.; Sharma, P.; Colley, H. E.; Murdoch, C.; Williams, D. P.; Webb, S. D. Characterization of a functional C3A liver spheroid model. *Toxicol. Res.* **2016**, *5* (4), 1053–1065.
- (6) Bachmann, A.; Moll, M.; Gottwald, E.; Nies, C.; Zantl, R.; Wagner, H.; Burkhardt, B.; Sánchez, J. J. M.; Ladurner, R.; Thasler, W.; et al. 3D Cultivation Techniques for Primary Human Hepatocytes. *Microarrays* **2015**, *4* (1), 64–83.
- (7) Usta, O.; McCarty, W.; Bale, S.; Hegde, M.; Jindal, R.; Bhushan, A.; Golberg, I.; Yarmush, M. Microengineered cell and tissue systems for drug screening and toxicology applications: Evolution of in-vitro liver technologies. *Technology* **2015**, *3* (01), 1–26.
- (8) Kang, Y. B. A.; Rawat, S.; Cirillo, J.; Bouchard, M.; Noh, H. M. Layered long-term co-culture of hepatocytes and endothelial cells on a transwell membrane: toward engineering the liver sinusoid. *Biofabrication* **2013**, *5* (4), 045008.
- (9) van Grunsven, L. A. 3D in vitro models of liver fibrosis. *Adv. Drug Delivery Rev.* **2017**, *121*, 133–146.
- (10) Kramer, N.; Walzl, A.; Unger, C.; Rosner, M.; Krupitza, G.; Hengstschläger, M.; Dolznig, H. In vitro cell migration and invasion assays. *Mutat. Res., Rev. Mutat. Res.* **2013**, *752* (1), 10–24.
- (11) Agarwal, T.; Narayan, R.; Maji, S.; Ghosh, S. K.; Maiti, T. K. Decellularized Caprine liver extracellular matrix as a 2D substrate coating and 3D hydrogel platform for vascularized liver tissue engineering. *J. Tissue Eng. Regener. Med.* **2018**, *12* (3), No. e1678-e1690.
- (12) Ng, K.; Gao, B.; Yong, K. W.; Li, Y.; Shi, M.; Zhao, X.; Li, Z.; Zhang, X.; Pingguan-Murphy, B.; Yang, H.; et al. Paper based cell culture platform and its emerging biomedical applications. *Mater. Today* **2017**, *20* (1), 32–44.
- (13) Agarwal, T.; Maiti, T. K.; Behera, B.; Ghosh, S. K.; Apoorva, A.; Padmavati, M. Biofunctionalized cellulose paper matrix for cell delivery applications. *Int. J. Biol. Macromol.* **2019**, *139*, 114–127.
- (14) Zhou, Y.; Fu, J. J.; Liu, Y. S.; Kang, Y. J.; Li, C. M.; Yu, L. Redefining Chinese calligraphy rice paper: an economical and cytocompatible substrate for cell biological assays. *RSC Adv.* **2017**, *7* (65), 41017–41023.
- (15) Lei, K. F.; Huang, C.-H. Paper-based microreactor integrating cell culture and subsequent immunoassay for the investigation of cellular phosphorylation. *ACS Appl. Mater. Interfaces* **2014**, *6* (24), 22423–22429.
- (16) Kenney, R. M.; Loeser, A.; Whitman, N. A.; Lockett, M. R. Paper-based Transwell assays: an inexpensive alternative to study cellular invasion. *Analyst* **2019**, *144* (1), 206–211.
- (17) Simon, K. A.; Mosadegh, B.; Minn, K. T.; Lockett, M. R.; Mohammady, M. R.; Boucher, D. M.; Hall, A. B.; Hillier, S. M.; Udagawa, T.; Eustace, B. K.; et al. Metabolic response of lung cancer cells to radiation in a paper-based 3D cell culture system. *Biomaterials* **2016**, *95*, 47–59.
- (18) Truong, A. S.; Lochbaum, C. A.; Boyce, M. W.; Lockett, M. R. Tracking the invasion of small numbers of cells in paper-based assays with quantitative PCR. *Anal. Chem.* **2015**, *87* (22), 11263–11270.
- (19) Kenney, R. M.; Boyce, M. W.; Truong, A. S.; Bagnell, C. R.; Lockett, M. R. Real-time imaging of cancer cell chemotaxis in paper-based scaffolds. *Analyst* **2016**, *141* (2), 661–668.
- (20) Derda, R.; Tang, S. K.; Laromaine, A.; Mosadegh, B.; Hong, E.; Mwangi, M.; Mammo, A.; Ingber, D. E.; Whitesides, G. M. Multizone paper platform for 3D cell cultures. *PLoS One* **2011**, *6* (5), No. e18940.
- (21) Fu, J. J.; Zhou, Y.; Shi, X. X.; Kang, Y. J.; Lu, Z. S.; Li, Y.; Li, C. M.; Yu, L. Spontaneous formation of tumor spheroid on a hydrophilic filter paper for cancer stem cell enrichment. *Colloids Surf., B* **2019**, *174*, 426–434.
- (22) Pupinyo, N.; Chatatikun, M.; Chiabchalar, A.; Laiwattanapaisal, W. In situ paper-based 3D cell culture for rapid screening of the antimelanogenic activity. *Analyst* **2019**, *144* (1), 290–298.
- (23) Wang, Y.; Su, W.; Wang, L.; Jiang, L.; Liu, Y.; Hui, L.; Qin, J. Paper supported long-term 3D liver co-culture model for the assessment of hepatotoxic drugs. *Toxicol. Res.* **2018**, *7* (1), 13–21.
- (24) Michael, I. J.; Kumar, S.; Oh, J. M.; Kim, D.; Kim, J.; Cho, Y.-K. Surface-Engineered Paper Hanging Drop Chip for 3D Spheroid Culture and Analysis. *ACS Appl. Mater. Interfaces* **2018**, *10* (40), 33839–33846.
- (25) Deiss, F. d. r.; Mazzeo, A.; Hong, E.; Ingber, D. E.; Derda, R.; Whitesides, G. M. Platform for high-throughput testing of the effect of soluble compounds on 3D cell cultures. *Anal. Chem.* **2013**, *85* (17), 8085–8094.

- (26) Agarwal, T.; Rustagi, A.; Das, J.; Maiti, T. K. PAMAM dendrimer grafted cellulose paper scaffolds as a novel in vitro 3D liver model for drug screening applications. *Colloids Surf, B* **2018**, *172*, 346–354.
- (27) Lei, K. F.; Liu, T.-K.; Tsang, N.-M. Towards a high throughput impedimetric screening of chemosensitivity of cancer cells suspended in hydrogel and cultured in a paper substrate. *Biosens. Bioelectron.* **2018**, *100*, 355–360.
- (28) Lei, K. F.; Huang, C.-H.; Tsang, N.-M. Impedimetric quantification of cells encapsulated in hydrogel cultured in a paper-based microchamber. *Talanta* **2016**, *147*, 628–633.
- (29) Lei, K. F.; Chang, C.-H.; Chen, M.-J. Paper/PMMA Hybrid 3D Cell Culture Microfluidic Platform for the Study of Cellular Crosstalk. *ACS Appl. Mater. Interfaces* **2017**, *9* (15), 13092–13101.
- (30) Trouillon, R.; Gijs, M. A. Dynamic electrochemical quantitation of dopamine release from a cells-on-paper system. *RSC Adv.* **2016**, *6* (37), 31069–31073.
- (31) Huang, C.-H.; Lei, K. F.; Tsang, N.-M. Paper-based microreactor array for rapid screening of cell signaling cascades. *Lab Chip* **2016**, *16* (15), 2911–2920.
- (32) Dey, R.; Kar, S.; Joshi, S.; Maiti, T. K.; Chakraborty, S. Ultra-low-cost ‘paper-and-pencil’ device for electrically controlled micromixing of analytes. *Microfluid. Nanofluid.* **2015**, *19* (2), 375–383.
- (33) Seluanov, A.; Vaidya, A.; Gorbunova, V. Establishing primary adult fibroblast cultures from rodents. *J. Visualized Exp.* **2010**, No. 44, No. e2033.
- (34) Cramer, S. M.; Larson, T. S.; Lockett, M. R. Tissue Papers: Leveraging paper-based microfluidics for the next generation of 3D tissue models. *Anal. Chem.* **2019**, *91* (17), 10916–10926.
- (35) Deiss, F.; Mattock, W. L.; Govindasamy, N.; Lin, E. Y.; Derda, R. Flow-through synthesis on Teflon-patterned paper to produce peptide arrays for cell-based assays. *Angew. Chem., Int. Ed.* **2014**, *53* (25), 6374–6377.
- (36) Mani, N. K.; Prabhu, A.; Biswas, S. K.; Chakraborty, S. Fabricating Paper Based Devices Using Correction Pens. *Sci. Rep.* **2019**, *9* (1), 1752.
- (37) Wang, L.; Xu, C.; Zhu, Y.; Yu, Y.; Sun, N.; Zhang, X.; Feng, K.; Qin, J. Human induced pluripotent stem cell-derived beating cardiac tissues on paper. *Lab Chip* **2015**, *15* (22), 4283–4290.
- (38) Juvonen, H.; Määttänen, A.; Laurén, P.; Ihälainen, P.; Urtti, A.; Yliperttula, M.; Peltonen, J. Biocompatibility of printed paper-based arrays for 2-D cell cultures. *Acta Biomater.* **2013**, *9* (5), 6704–6710.
- (39) Wang, M.; Wang, Y.; Gao, B.; Bian, Y.; Liu, X.; He, Z.; Zeng, Y.; Du, X.; Gu, Z. Fast Strategy to Functional Paper Surfaces. *ACS Appl. Mater. Interfaces* **2019**, *11* (15), 14445–14456.
- (40) Shahin-Shamsabadi, A.; Selvaganapathy, P. R. ExCeL: combining extrusion printing on cellulose scaffolds with lamination to create in vitro biological models. *Biofabrication* **2019**, *11* (3), 035002.
- (41) Camp, J. P.; Capitano, A. T. Induction of zone-like liver function gradients in HepG2 cells by varying culture medium height. *Biotechnol. Prog.* **2007**, *23* (6), 1485–1491.
- (42) Nishikawa, T.; Tanaka, Y.; Nishikawa, M.; Ogino, Y.; Kusamori, K.; Mizuno, N.; Mizukami, Y.; Shimizu, K.; Konishi, S.; Takahashi, Y.; et al. Optimization of albumin secretion and metabolic activity of cytochrome P450 1A1 of human hepatoblastoma HepG2 cells in multicellular spheroids by controlling spheroid size. *Biol. Pharm. Bull.* **2017**, *40* (3), 334–338.
- (43) Ranucci, C. S.; Kumar, A.; Batra, S. P.; Moghe, P. V. Control of hepatocyte function on collagen foams: sizing matrix pores toward selective induction of 2-D and 3-D cellular morphogenesis. *Biomaterials* **2000**, *21* (8), 783–793.
- (44) Holownia, A.; Braszko, J. J. Acetaminophen alters microsomal ryanodine Ca²⁺ channel in HepG2 cells overexpressing CYP2E1. *Biochem. Pharmacol.* **2004**, *68* (3), 513–521.
- (45) Prot, J. M.; Briffaut, A.-S.; Letourneur, F.; Chafey, P.; Merlier, F.; Grandvalet, Y.; Legallais, C.; Leclerc, E. Integrated proteomic and transcriptomic investigation of the acetaminophen toxicity in liver microfluidic biochip. *PLoS One* **2011**, *6* (8), No. e21268.
- (46) Aritomi, K.; Ishitsuka, Y.; Tomishima, Y.; Shimizu, D.; Abe, N.; Shuto, T.; Irikura, M.; Kai, H.; Irie, T. Evaluation of three-dimensional cultured HepG2 cells in a nano culture plate system: an in vitro human model of acetaminophen hepatotoxicity. *J. Pharmacol. Sci.* **2014**, *124* (2), 218–229.
- (47) Ramaiahgari, S. C.; Den Braver, M. W.; Herpers, B.; Terpstra, V.; Commandeur, J. N.; van de Water, B.; Price, L. S. A 3D in vitro model of differentiated HepG2 cell spheroids with improved liver-like properties for repeated dose high-throughput toxicity studies. *Arch. Toxicol.* **2014**, *88* (5), 1083–1095.
- (48) Bale, S. S.; Golberg, I.; Jindal, R.; McCarty, W. J.; Luitje, M.; Hegde, M.; Bhushan, A.; Usta, O. B.; Yarmush, M. L. Long-term coculture strategies for primary hepatocytes and liver sinusoidal endothelial cells. *Tissue Eng., Part C* **2015**, *21* (4), 413–422.
- (49) Kostadinova, R.; Boess, F.; Applegate, D.; Suter, L.; Weiser, T.; Singer, T.; Naughton, B.; Roth, A. A long-term three dimensional liver co-culture system for improved prediction of clinically relevant drug-induced hepatotoxicity. *Toxicol. Appl. Pharmacol.* **2013**, *268* (1), 1–16.
- (50) Tetsuka, K.; Ohbuchii, M.; Tabata, K. Recent progress in hepatocyte culture models and their application to the assessment of drug metabolism, transport, and toxicity in drug discovery: the value of tissue engineering for the successful development of a microphysiological system. *J. Pharm. Sci.* **2017**, *106* (9), 2302–2311.
- (51) Lee, H. W.; Kook, Y.-M.; Lee, H. J.; Park, H.; Koh, W.-G. A three-dimensional co-culture of HepG2 spheroids and fibroblasts using double-layered fibrous scaffolds incorporated with hydrogel micro-patterns. *RSC Adv.* **2014**, *4* (105), 61005–61011.
- (52) Cui, J.; Wang, H.; Shi, Q.; Sun, T.; Huang, Q.; Fukuda, T. Multicellular Co-Culture in Three-Dimensional Gelatin Methacryloyl Hydrogels for Liver Tissue Engineering. *Molecules* **2019**, *24* (9), 1762.
- (53) Nelson, L. J.; Navarro, M.; Treskes, P.; Samuel, K.; Tura-Ceide, O.; Morley, S. D.; Hayes, P. C.; Plevritis, J. N. Acetaminophen cytotoxicity is ameliorated in a human liver organotypic coculture model. *Sci. Rep.* **2015**, *5*, 17455.
- (54) Navarro, M.; Nelson, L.; Treskes, P.; Samuel, K.; Plevritis, J. Hepatocytes improve their drug metabolic activity with the presence of endothelial cells in an in vitro hepatic co-culture model of acetaminophen toxicity. *J. Hepatol.* **2014**, *60* (1), S179.
- (55) Alshareeda, A. T.; Sakaguchi, K.; Abumaree, M.; Zin, N. K. M.; Shimizu, T. The potential of cell sheet technique on the development of hepatocellular carcinoma in rat models. *PLoS One* **2017**, *12* (8), No. e0184004.
- (56) Yang, Y.; Li, J.; Pan, X.; Zhou, P.; Yu, X.; Cao, H.; Wang, Y.; Li, L. Co-culture with mesenchymal stem cells enhances metabolic functions of liver cells in bioartificial liver system. *Biotechnol. Bioeng.* **2013**, *110* (3), 958–968.
- (57) Rebelo, S. P.; Costa, R.; Silva, M. M.; Marcelino, P.; Brito, C.; Alves, P. M. Three-dimensional co-culture of human hepatocytes and mesenchymal stem cells: improved functionality in long-term bioreactor cultures. *J. Tissue Eng. Regener. Med.* **2017**, *11* (7), 2034–2045.
- (58) Damania, A.; Jaiman, D.; Teotia, A. K.; Kumar, A. Mesenchymal stromal cell-derived exosome-rich fractionated secretome confers a hepatoprotective effect in liver injury. *Stem Cell Res. Ther.* **2018**, *9* (1), 31.
- (59) Huang, Y.; Ezquer, F.; Israel, Y.; Ezquer, M. Evaluation in vitro of the therapeutic effect of mesenchymal stem cell-conditioned medium on drug induced liver injury. *Cyotherapy* **2017**, *19* (5), S230.
- (60) Khawar, I. A.; Park, J. K.; Jung, E. S.; Lee, M. A.; Chang, S.; Kuh, H.-J. Three dimensional mixed-cell spheroids mimic stroma-mediated chemoresistance and invasive migration in hepatocellular carcinoma. *Neoplasia* **2018**, *20* (8), 800–812.
- (61) Wu, D. Signaling mechanisms for regulation of chemotaxis. *Cell Res.* **2005**, *15* (1), 52.
- (62) Keenan, T. M.; Folch, A. Biomolecular gradients in cell culture systems. *Lab Chip* **2008**, *8* (1), 34–57.
- (63) Fiore, E. J.; Domínguez, L. M.; Bayo, J.; García, M. G.; Mazzolini, G. D. Taking advantage of the potential of mesenchymal stromal cells in liver regeneration: Cells and extracellular vesicles as therapeutic strategies. *World J. Gastroenterol.* **2018**, *24* (23), 2427.

- (64) Fu, X.; Liu, G.; Halim, A.; Ju, Y.; Luo, Q.; Song, G. Mesenchymal Stem Cell Migration and Tissue Repair. *Cells* **2019**, *8* (8), 784.
- (65) Liau, L. L.; Makpol, S.; Azurah, A. G. N.; Chua, K. H. Human adipose-derived mesenchymal stem cells promote recovery of injured HepG2 cell line and show sign of early hepatogenic differentiation. *Cytotechnology* **2018**, *70* (4), 1221–1233.
- (66) Zhang, R.; Pan, X.; Huang, Z.; Weber, G. F.; Zhang, G. Osteopontin enhances the expression and activity of MMP-2 via the SDF-1/CXCR4 axis in hepatocellular carcinoma cell lines. *PLoS One* **2011**, *6* (8), No. e23831.
- (67) Teshima, T.; Matsumoto, H.; Koyama, H. Soluble factors from adipose tissue-derived mesenchymal stem cells promote canine hepatocellular carcinoma cell proliferation and invasion. *PLoS One* **2018**, *13* (1), No. e0191539.
- (68) Wilson, D. J.; Kumar, A. A.; Mace, C. R. Overreliance on Cost Reduction as a Featured Element of Sensor Design. *ACS Sens.* **2019**, *4* (5), 1120–1125.

■ NOTE ADDED AFTER ASAP PUBLICATION

This paper was published ASAP on March 30, 2020, with an incorrect Figure 5. The corrected version was posted on April 20, 2020.